

Evidence of strong interchannel coupling in Hg $5d$ photoionization by "experimental" transition matrix elements

G. Schönhense and U. Heinzmann

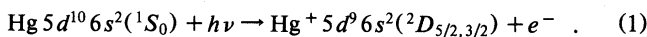
Fritz-Haber-Institut der Max-Planck-Gesellschaft, Faradayweg 4-6, D-1000 Berlin 33, West Germany

(Received 16 November 1983)

Experimental data of photoionization cross sections, photoelectron angular distributions, and photoelectron spin polarizations for mercury $5d$ have been used to determine dipole transition amplitudes and their relative phases. These basic quantities are compared with predictions of different theoretical models, revealing a strong interchannel interaction between the $5d \rightarrow \epsilon p$ and $5d \rightarrow \epsilon f$ channels, which was not directly visible in the measurable parameters.

Photoionization dynamics for high- Z atoms has received much attention within the last few years, mainly because it is characterized by an interesting interplay between relativistic (essentially spin-orbit) effects on the one side and many-electron correlations on the other side. Subject to such influences are all experimentally accessible quantities, such as the total photoionization cross section and branching ratios of partial cross sections, but also properties of the photoproducts such as the angular distribution and spin polarization of the photoelectrons or the alignment and orientation of the photoions. The quantitative response of the observables on relativistic and correlation effects is, however, very subtle because they are rather complex functions of the *basic* quantities that govern photoionization dynamics—namely, the transition matrix elements and their relative phases.¹ In order to analyze the given influences most clearly, it is therefore advantageous to consider the basic quantities directly. From the experimental point of view this requires a number of independent measurements, which equals the number of basic quantities involved.² It is the purpose of this article to present the results obtained from such an analysis for ionization of the (inner) $5d^{10}$ subshell of mercury together with *ab initio* calculations in different models (Hartree-Fock, Dirac-Slater, random-phase approximation). This example verifies experimentally that interchannel coupling between different photoionization channels from one subshell ($5d \rightarrow \epsilon p$ and $5d \rightarrow \epsilon f$) may lead to a conspicuous effect in the dipole transition amplitudes and phase-shift differences of continuum wave functions.

The present investigation has been made for the Hg $5d$ subshell because mercury ($Z=80$) is a heavy element, showing strong spin-orbit coupling, and because photoionization of the (inner) $5d^{10}$ subshell should exhibit influences of many-electron correlations. The analyzed reaction reads



Spin-orbit interaction causes a fine-structure splitting of 1.86 eV between the 2D final ionic states, which can be easily resolved by means of photoelectron spectroscopy. For this process experimental information exists concerning photoionization cross sections as well as photoelectron angular distributions and spin polarizations. From the total photoionization cross section³ and the branching ratios⁴ follows the partial cross section Q_j for the production of the 2D final ionic states with $j = \frac{5}{2}$ and $\frac{3}{2}$. Furthermore, the angular distribution of photoelectrons has been investigated yielding the asymmetry parameter β_j (Ref. 5) of the differential

cross section:

$$\frac{d\sigma_j}{d\Omega}(\theta) = \frac{Q_j}{4\pi} \left[1 - \frac{1}{2} \beta_j P_2(\cos\theta) \right] \quad (2)$$

Finally, the photoelectron spin-polarization component normal to the reaction plane,

$$P_{\perp j}(\theta) = \xi_j \sin 2\theta / \left[1 - \frac{1}{2} \beta_j P_2(\cos\theta) \right] \quad (3)$$

has been measured at the magic angle [$P_2(\cos\theta_m) = 0$] yielding the spin parameter ξ_j .⁶ The angular terms $\sin 2\theta$ and $P_2(\cos\theta) = \frac{3}{2} \cos^2\theta - \frac{1}{2}$ in Eqs. (2) and (3) reflect the simple geometry of photoemission after a bound-free dipole transition from a spherically symmetric atomic state. The information about photoionization dynamics is contained in the parameters Q_j , β_j , and ξ_j .

In the framework of the *jj*-coupling scheme, Eq. (1) represents three transition-matrix elements for each of the final ionic states (i.e., $5d_{5/2} \rightarrow \epsilon p_{3/2}$, $\epsilon f_{5/2}$, $\epsilon f_{7/2}$, and $5d_{3/2} \rightarrow \epsilon p_{1/2}$, $\epsilon p_{3/2}$, $\epsilon f_{5/2}$), according to the dipole selection rules. Since only relative phases, i.e., phase differences, are observable, the resulting number of independent parameters is five for both subshells. This is in contrast to the photoionization of the np^6 valence shells of rare gases studied recently,⁷ where for $j = \frac{1}{2}$ only two transition amplitudes ($np_{1/2} \rightarrow \epsilon s_{1/2}$, $\epsilon d_{3/2}$) plus one relative phase, i.e., three independent parameters, appear. The three experimental quantities Q_j , β_j , and ξ_j for Hg $5d$ do not permit an evaluation applying *jj*-coupling formulas; however, they do permit an analysis using *LS*-coupling equations. In this approximation, also referred to as the Cooper-Zare model, the difference between $\epsilon f_{5/2}$ and $\epsilon f_{7/2}$ as well as $\epsilon p_{1/2}$ and $\epsilon p_{3/2}$ is neglected, so that Eq. (1) simply represents the two transitions $5d \rightarrow \epsilon p$, ϵf described by the radial matrix elements R_p and R_f and the phase-shift difference $\delta_f - \delta_p$. The three relevant parameters follow from the general theoretical treatments:¹

$$Q_{5/2} = 4\pi^2 \alpha a_0^2 \omega \frac{6}{15} (2R_p^2 + 3R_f^2) = 6(Q_{5/2}^p + Q_{5/2}^f) \quad (4)$$

$$Q_{3/2} = 4\pi^2 \alpha a_0^2 \omega \frac{4}{15} (2R_p^2 + 3R_f^2) = 4(Q_{3/2}^p + Q_{3/2}^f) \quad (4)$$

$$\beta_{5/2} = \frac{12R_f^2 + 2R_p^2 - 36R_f R_p \cos(\delta_f - \delta_p)}{15R_f^2 + 10R_p^2} \quad (5)$$

$$\beta_{3/2} = \text{same expression with } f'p' \quad (5)$$

$$\xi_{5/2} = -\frac{3R_f R_p \sin(\delta_f - \delta_p)}{6R_f^2 + 4R_p^2} \quad (6)$$

$$\xi_{3/2} = \frac{9R_f R_p \sin(\delta_f - \delta_p)}{12R_f^2 + 8R_p^2} \quad (6)$$

It should be mentioned that *LS*-coupling theory cannot distinguish between primed and unprimed quantities, with the consequence that $Q_{5/2}^{LS} = 1.5 Q_{3/2}^{LS}$; $\xi_{3/2}^{LS} = -1.5 \xi_{5/2}^{LS}$, and $\beta_{3/2}^{LS} = \beta_{5/2}^{LS}$. This does not mean, however, that in the application of the Cooper-Zare model any influences of spin-orbit interaction are neglected *a priori*—otherwise no photoelectron spin polarization could be predicted using this model (see Cherepkov¹). Only spin-orbit interaction in the electronic continuum is not taken into account. Experimentally, the separation of electrons corresponding to $j = \frac{5}{2}$ and $\frac{3}{2}$ is made by means of the electron spectrometer selecting either the $^2D_{5/2}$ or the $^2D_{3/2}$ final ionic state, so that our analysis does distinguish between the spin-orbit components. The structure of the spin parameter ξ_j is noticeable: It is given by only an interference term containing the ratio of the two amplitudes and the sine of the corresponding phase-shift difference, demonstrating its high sensitivity upon the relative phase.

Using Eqs. (4)–(6) the matrix elements and relative phases have been deduced from the experimental values of Q_j ,^{3,4} β_j ,⁵ and ξ_j .⁶ An unambiguous determination of the phase difference was possible, because it enters into the equations of condition as the argument of both sine and cosine functions. The results are shown in Figs. 1–3; the

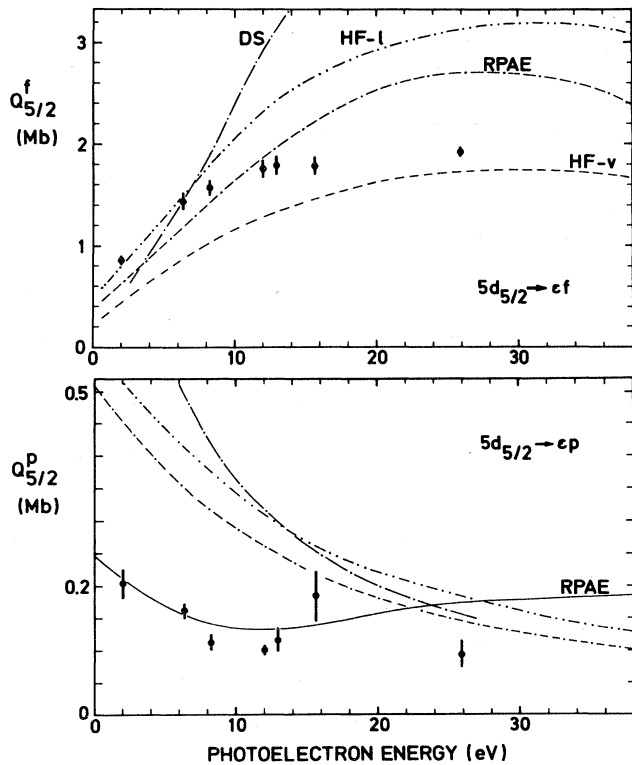


FIG. 1. Partial cross section per electron for the $5d \rightarrow \epsilon f$ and $5d \rightarrow \epsilon p$ channels (upper and lower part, respectively) with the photoion left in its final state $Hg^{+2}D_{5/2}$. Theoretical predictions: \cdots Hartree-Fock (length form), Ref. 8; $---$ Hartree-Fock (velocity form), Ref. 8; $-\cdot-\cdot-$ Dirac-Slater, Ref. 9; $-\cdot-\cdot-$ RPAE with many-electron corrections within one channel only, Ref. 8; $---$ RPAE with intertransition correlations between $5d \rightarrow \epsilon p$ and $5d \rightarrow \epsilon f$, Ref. 8.

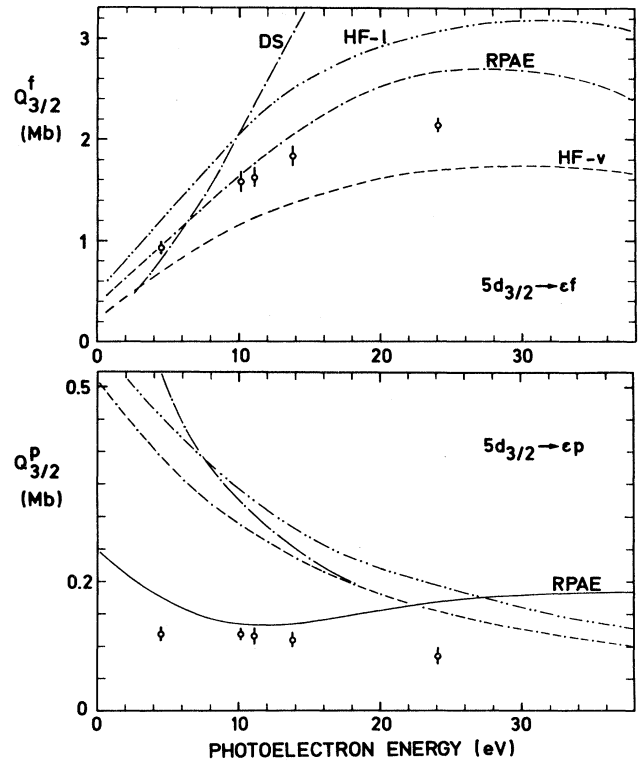


FIG. 2. The same as in Fig. 1 but with the photoion left in its final state $Hg^{+2}D_{3/2}$.

error bars given include the errors of the three different measurements. β_j and ξ_j have been measured using discharge light sources; therefore, the corresponding photon energies are resonance lines of helium and neon.⁵ The partial cross sections per electron Q_j^f (Figs. 1 and 2) represent the squared matrix elements apart from a constant factor, defined by Eq. (4). The basic quantities given in the figures show that the energy dependence of the dynamical pho-

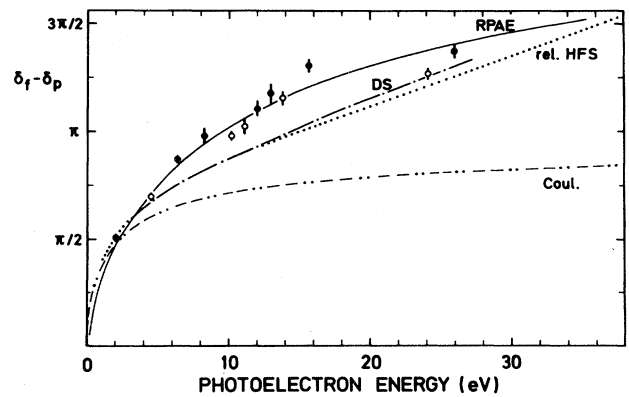


FIG. 3. Phase-shift difference between the ϵf and the ϵp partial wave. Full and open symbols correspond to $j = \frac{5}{2}$ and $\frac{3}{2}$, respectively. Theoretical predictions as in Fig. 1, except for the following: \cdots relativistic Hartree-Slater, Ref. 10; $---$ Coulomb-phase difference $\sigma_f - \sigma_p - \pi$.

toionization parameters is qualitatively characterized by the following features: Close to threshold the difference of the Coulomb-scattering phase $\sigma_f - \sigma_p$ (cf. Fig. 3) varies rapidly. This contribution to the total phase difference $\delta_f - \delta_p$ is known analytically.¹¹ Within the kinetic energy interval $E_{\text{kin}} = 0$ to 2.3 eV the Coulomb-phase difference changes by $\pi/2$, which is already half the total change between $E_{\text{kin}} = 0$ and ∞ . A consequence is the strong variation of the phase-dependent parameters at small energies (cf. Refs. 5 and 6). At higher energies a delayed maximum in the matrix element of the $nd \rightarrow \epsilon f$ channel appears (upper parts of Figs. 1 and 2). The origin of this delayed onset of the cross section is the angular-momentum barrier in the effective potential, which prevents the ϵf continuum orbital from penetrating into the barrier region at small energies.¹¹ For some elements this feature exhibits pronounced resonance character (shape resonance), associated with a change by π in the phase difference. At higher energies (not shown in the figures), the shape resonance is followed by a Cooper minimum in the same channel. These three characteristics—the variation of the Coulomb-phase difference, the delayed onset of the cross section, and the Cooper minimum—are predicted qualitatively already in a nonrelativistic single-particle model.¹¹ However, in order to reach a quantitative understanding it is necessary to take into account relativistic and many-electron effects.

The main effect of relativistic corrections is to introduce a difference between wave functions with total angular momenta $l + \frac{1}{2}$ and $l - \frac{1}{2}$. A result of this difference shows up in the transition matrix elements corresponding to the final ionic states $^2D_{5/2}$ and $^2D_{3/2}$ (Figs. 1 and 2, respectively). Especially the $5d \rightarrow \epsilon p$ partial cross sections (lower parts) differ considerably—in contrast to the nonrelativistic prediction $Q_{5/2}^l = Q_{3/2}^l$. Also the measured phase-shift difference is consistently higher for $^2D_{5/2}$ than for $^2D_{3/2}$.

A most striking effect of many-electron correlations can be seen in the experimental matrix elements for the weak $l \rightarrow l-1$ transition: While single-electron calculations (Hartree-Fock and Dirac-Slater) predict a monotonically decreasing curve, with relatively high values close to threshold, the experimental points show a minimum around 10 eV for $^2D_{5/2}$ and only a very weak energy dependence for $^2D_{3/2}$. Experiment is, however, rather close to the prediction of the random-phase approximation (RPAE).⁸ This calculation starts from Hartree-Fock single-electron approximation and adds many-electron corrections within the $5d \rightarrow \epsilon p$ channel (double-dash dot) and intertransition correlations¹² between $5d \rightarrow \epsilon p$ and $5d \rightarrow \epsilon f$ (full curve). These latter correlations, i.e., the influences of the strong $5d \rightarrow \epsilon f$ transition upon the weak $5d \rightarrow \epsilon p$ transition, drastically reduce the $5d \rightarrow \epsilon p$

matrix element at low photon energies down to a flat minimum around 10 eV. The shape-resonance maximum in the $l \rightarrow l+1$ channel (around 30 eV) reflects itself also in the weak $l \rightarrow l-1$ transition amplitude, demonstrating the strong interchannel coupling in Hg 5d photoionization. For the phase-shift difference, the inclusion of interchannel interactions results in a faster increase than predicted by uncorrelated (Dirac-Slater and relativistic Hartree-Slater) theories. The experimental values of $\delta_f - \delta_p$ confirm this faster increase.

There still remain systematic differences between the RPAE and experiment, in particular regarding the matrix elements. Being a nonrelativistic theory, the RPAE is not able to explain the difference between full and open symbols (i.e., final ionic states $^2D_{5/2}$ and $^2D_{3/2}$). The predicted maximum of the $5d \rightarrow \epsilon f$ transition amplitudes is too high, which is the case for nearly all calculations available,^{8-10,13} and also the $5d \rightarrow \epsilon p$ amplitudes do not agree quantitatively with experiment. This is a consequence not only of the neglect of spin-orbit interaction but also of correlations with electrons of other subshells. The (open) channel of valence-shell ionization $6s \rightarrow \epsilon p$, for example, should give a non-negligible contribution. A recent relativistic RPA calculation¹³ takes $6s$ ionization into account, but—as pointed out before—the number of experimental quantities available at present does not permit an evaluation employing the jj -coupling scheme.

In summary, our analysis of mercury 5d photoionization in the region of the delayed onset of the $5d \rightarrow \epsilon f$ partial cross section has experimentally verified that interchannel interactions in the continuum can have a large quantitative influence upon transition-matrix elements and their relative phases. This type of correlation between transition channels from one subshell into different continua (the so-called intertransition correlation) was sometimes considered to be weak as compared with other many-electron effects, e.g., interactions between transitions starting from different subshells (intershell correlations). The analysis performed in terms of experimental matrix elements and phase differences in comparison with theoretical results offered the advantage that relativistic and correlation effects could be observed most directly, whereas the measurable parameters are rather complex functions of these basic quantities.

We would like to thank Professor J. Kessler for his interest and support and Dr. N. A. Cherepkov for helping us to understand the Russian manuscript of Ref. 8. Financial support by the Deutsche Forschungsgemeinschaft is gratefully acknowledged.

¹See, e.g., N. A. Cherepkov, Zh. Eksp. Teor. Fiz. **65**, 933 (1973) [Sov. Phys. JETP **38**, 463 (1974)]; C. M. Lee, Phys. Rev. A **10**, 1598 (1974); and K.-N. Huang, W. R. Johnson, and K. T. Cheng, At. Data Nucl. Data Tables **26**, 33 (1981).

²In this context the expression "complete experiment" is frequently used. It must be pointed out, however, that an experiment can only be complete within a particular model, i.e., making certain approximations, e.g., the application of the LS -coupling scheme, the dipole approximation, the neglect of hyperfine interactions, etc.

³R. B. Cairns, H. Harrison, and R. I. Schoen, J. Chem. Phys. **53**, 96 (1970); J. L. Dehmer and J. Berkowitz, Phys. Rev. A **10**, 484 (1974).

⁴S. P. Shannon and K. Codling, J. Phys. B **11**, 1193 (1978).

⁵G. Schönhense, J. Phys. B **14**, L187 (1981).

⁶G. Schönhense, F. Schäfers, U. Heinzmann, and J. Kessler, Z. Phys. A **304**, 31 (1982).

⁷U. Heinzmann, J. Phys. B **13**, 4353 (1980); **13**, 4367 (1980); F. Schäfers, G. Schönhense, and U. Heinzmann, Phys. Rev. A **28**, 802 (1983).

- ⁸V. K. Ivanov, S. Yu. Medvedev, and V. A. Sosnivker, A. F. Ioffe Physical-Technical Institute, Leningrad, Report No. 615, 1979 (unpublished).
- ⁹F. Keller and F. Combet-Farnoux, *J. Phys. B* 12, 2821 (1979); 15, 2657 (1982); (private communication).
- ¹⁰Y. S. Kim, R. H. Pratt, A. Ron, and H. K. Tseng, *Phys. Rev. A* 22, 567 (1980).
- ¹¹See, e.g., A. F. Starace, in *Handbuch der Physik*, edited by W. Mehlhorn (Springer, Berlin, 1982), Vol. 31.
- ¹²M. Ya. Amusia, *Comm. At. Mol. Phys.* 8, 61 (1979).
- ¹³W. R. Johnson, V. Radojevic, K. P. Deshmukh, and K. T. Cheng, *Phys. Rev. A* 25, 337 (1982).